Evaluation of Theoretical, Semi-Empirical, and Empirical Approaches for Determining K-Shell Absorption Parameters for Elements with Z = 18–100.

I. Hamied[1,2], A. Kahoul[1,2*], E. Cengiz[3], J.P. Marques[4,5], S. Daoudi[1,2], F. Parente[4], J.M. Sampaio[5,6], S. Croft[7], A. Favalli[8,9], Y. Kasri[10,11]

[1]*Department of Matter Sciences, Faculty of Sciences and Technology, Mohamed El Bachir El Ibrahimi University, Bordj-Bou-Arreridj 34030, Algeria.*
[2]*Laboratory of Materials Physics,Radiation and Nanostructures (LPMRN), Faculty of Sciences and Technology, University of Mohamed El Bachir El Ibrahimi, Bordj-Bou-Arreridj 34030, Algeria.*
[3]*Department of Fundamental Sciences, Rafet Kayış Engineering Faculty, Alanya Alaaddin Keykubat University, 07425 Alanya/Antalya, Türkiye*
[4]*LIP – Laboratório de Instrumentação e Física Experimental de Partículas, Av. Prof. Gama Pinto 2, 1649-003 Lisboa, Portugal.*
[5]*Faculdade de Ciências da Universidade de Lisboa, Campo Grande, C8, 1749-016 Lisboa, Portugal.*
[6]*Laboratory of Instrumentation, Biomedical Engineering and Radiation Physics (LIBPhys-UNL), Department of Physics, NOVA School of Science and Technology, NOVA University Lisbon, 2829-516 Caparica, Portugal.*
[7]*School of Engineering, Faculty of Science of Technology, Nuclear Science & Engineering Research Group, Lancaster University, Bailrigg, Lancaster, LA1 4YW, United Kingdom.*
[8]*European Commission, Joint Research Centre, Ispra, I-21027, Italy.*
[9]*Los Alamos National Laboratory, P.O. Box 1663, Los Alamos, NM 87545, USA.*
[10]*Physics Department, Faculty of Sciences, University of Mohamed Boudiaf, 28000 M'sila, Algeria.*
[11]*Theoretical Physics Laboratory, Faculty of Exact Sciences, University of Bejaia, 06000 Bejaia, Algeria.*

[*]Corresponding author. Tel. /Fax (+213) 035862230.
E-mail address: *a.kahoul@univ-bba.dz*

Abstract

This study presents a comprehensive evaluation of K-shell absorption parameters for elements with atomic numbers ranging from 18 to 100. The focus is on key parameters such as the absorption jump ratio, the absorption jump factor, the Davisson–Kirchner ratio, and the oscillator strength. The accuracy and reliability of these parameters are critically assessed using analytical, experimental, and theoretical approaches. Experimental values are compiled based on a thorough review of current literature, while theoretical values are calculated using established computational models such as XCOM and FFAST. Analytical estimations are derived through a combination of empirical and semi-empirical methods, aiming to explain systematic trends and correlations between absorption properties and atomic numbers. The findings provide valuable insights into K-shell absorption mechanisms and underscore the importance of accurate parameterization in advancing the understanding of X-ray absorption physics.

Keywords: K-shell absorption, X-ray absorption, absorption jump ratio, absorption jump factor, Davisson-Kirchner ratio, oscillator strength.

I. Introduction

The study of K-shell absorption parameters is crucial for advancing our understanding of X-ray interactions with matter, with important implications for diverse fields such as X-ray spectroscopy, materials science, and medical physics. These parameters, including the absorption jump ratio, the jump factor, the Davisson-Kirchner (DK) ratio, and the oscillator strength, characterize the discontinuities observed in absorption coefficients at the K-edge. Accurate determination of these values is essential for a wide range of applications, such as elemental analysis, the development of radiation shielding materials, and the optimization of diagnostic imaging protocols (Budak and Polat, 2004; Polat et al., 2013; Akman, 2015; Ekanayake, 2021).

The present study provides a comprehensive evaluation of theoretical models, experimental measurements, and both empirical and semi-empirical approaches used to determine K-shell absorption parameters. A systematic comparison of these methodologies is essential to resolve existing discrepancies and to enhance the overall understanding of X-ray absorption phenomena.

The mass attenuation coefficient μ/ρ is a fundamental quantity that describes the probability of photon interactions with matter, incorporating contributions from photoelectric absorption, Compton scattering, and pair production. The predominance of each interaction mechanism depends on both the photon energy and the atomic number Z of the target element. At low X-ray photon energies, photoelectric absorption is the dominant process, while Compton scattering becomes more significant at intermediate energies. Pair production, by contrast, occurs only when photon energies exceed approximately 1.02 MeV. When μ/ρ values are plotted as a function of photon energy, they typically exhibit a characteristic sawtooth pattern near the K-shell binding energy, indicating a sudden increase in absorption due to K-shell electron involvement. This distinctive feature underscores the photoelectric effect as the

primary mechanism responsible for low-energy photon attenuation, particularly in the region just above the binding energy threshold.

Extensive research has produced a substantial body of photon cross-section data. Foundational contributions include the tabulations by Scofield (1973) and Chantler (1995), the XCOM database developed by Berger et al. (2010), and the FFAST compilation by Chantler et al. (2005). In recent years, to further refine atomic parameters, integrated approaches combining experimental, theoretical, and computational methods have been employed. For example, experimental investigations into K-shell jump ratios and jump factors have been carried out by Ayala and Mainardi (1996) for erbium, Budak and Polat (2004) for gadolinium, dysprosium, holmium, and erbium, and Kaya et al. (2007) for thulium, ytterbium, lutetium, hafnium, tantalum, tungsten, rhenium, and osmium. Further contributions include studies by Polat et al. (2005, 2013), Bennal and Badiger (2007), and Sidhu et al. (2011), which focused on mass attenuation coefficients and K-shell parameters across a range of elements.

Numerous studies have investigated attenuation cross-sections, oscillator strengths, and Davisson-Kirchner (DK) ratios, using radioactive sources such as ^{241}Am and ^{109}Cd in combination with photon detectors like Si(Li). Early contributions include the works of Mallikarjuna et al. (2002) and Hosur et al. (2008, 2011). Subsequent research by Akman et al. (2015a) and Kaçal et al. (2015) further advanced this area. More recently, studies by Niranjana et al. (2013) and Akman et al. (2015b, 2016a) have extended these investigations to elements such as silver, cerium, and samarium.

In cases where experimental limitations arise (particularly for heavy elements), empirical and semi-empirical computational methods have proven essential for refining theoretical predictions and filling gaps. For example, Berkani et al. (2025) calculated vacancy transfer probabilities, while recent analyses by Zidi et al. (2025) emphasize the reliability of these approaches in determining X-ray fluorescence yields and intensity ratios. A broader overview

of empirical and semi-empirical methodologies can be found in the works of Kahoul et al. (2014), Sahnoun et al. (2016), Daoudi et al. (2020), Hamidani et al. (2023), Meddouh et al. (2023), Amari et al. (2024), Zidi et al. (2024), and Berkani et al. (2025).

Early empirical efforts to determine jump factors and jump ratios were conducted by researchers such as Rindfleisch (1937), Veigele (1973), Puttaswamy (1981), Broll (1986), Poehn et al. (1985), and Mallikarjuna et al. (2002).

This study applies a range of mathematical techniques, informed by both experimental and theoretical data, to investigate K-shell absorption parameters for elements with atomic numbers Z ranging from 18 to 100 for the jump ratio, and from 22 to 100 for the jump factor. The results show strong agreement with existing experimental observations and theoretical models, contributing to the refinement of atomic interaction data relevant to a wide range of scientific and technological applications.

The present study does not extend to lighter elements ($Z < 18$), for which the of K-shell absorption parameters in the soft X-ray region indeed requires distinct experimental and theoretical approaches compared to higher-Z elements. For light elements like oxygen, nitrogen, and carbon, the K-edges fall below ~1 keV - where soft X-rays are strongly attenuated by air. Consequently, measurements must be conducted in one of the following environments: ultrahigh vacuum, helium atmosphere, or using specialized gas-window chambers to avoid absorption by air and window materials Stohr. (1992), Stöhr and Outka. (1987). Experimental detection typically relies on fluorescence yield or electron yield techniques (e.g., total electron yield, TEY), as opposed to transmission geometry used more commonly in hard X-ray studies of heavier elements ($Z \geq 18$) Koningsberger and Prins. (1988). These soft X-ray studies also require synchrotron radiation due to the need for tunable, intense soft X-ray beams, alongside instrumentation such as monochromators, vacuum or helium chambers, and detectors optimized for low-energy photons Ade and Hitchcock. (2008). Theoretically, the near-edge

region is dominated by multiple-scattering resonances, short photoelectron mean free paths (on the order of ~ 0.3 nm at ~50 eV), and strong excitonic or many-body effects-necessitating models based on NEXAFS (Near Edge X-ray Absorption Fine Structure) rather than EXAFS Stöhr. (1992). In contrast, for hard X-rays (Z≥18), traditional transmission or fluorescence/attenuation approaches with thicker samples are sufficient, and modeling focuses on EXAFS/XANES frameworks without the pronounced near-edge complexity.

II. Theoretical background and data analysis

This section focuses on key theoretical concepts and analytical methodologies used to characterize material behavior for K-shell electrons. Specifically, it examines the absorption jump ratio, the absorption jump factor, the Davisson–Kirchner ratio, and the oscillator strength. Together, these parameters provide valuable insights into the electronic structure of materials and quantify the probabilities associated with various X-ray interaction mechanisms.

1. K-shell absorption jump ratio

The absorption edge jump ratio r_{K} is defined as the ratio of the total attenuation cross-section just above the absorption edge (σ_a) to that just below the edge (σ_b). It can be calculated using the following relation (Niranjana et al. 2013):

$$r_{\mathrm{K}} = \frac{\tau_{\mathrm{K}}+\tau_{\mathrm{L}}+\tau_{\mathrm{M}}+\cdots\ldots\ldots+\sigma_{\mathrm{coh}}+\sigma_{\mathrm{incoh}}}{\tau_{\mathrm{L}}+\tau_{\mathrm{M}}+\cdots\ldots\ldots+\sigma_{\mathrm{coh}}+\sigma_{\mathrm{incoh}}} = \frac{\sigma_{\mathrm{a}}}{\sigma_{\mathrm{b}}} \qquad (3)$$

where $\tau_{\mathrm{K}}, \tau_{\mathrm{L}}$ and τ_{M} are the K, L and M shell photoelectric cross sections, and σ_{coh} is the coherent (the Rayleigh) scattering cross-section and σ_{incoh} is the incoherent (the Compton) scattering cross-section. At the absorption edge of the material under investigation, the photoelectric effect is the dominant interaction mechanism, while the contribution of scattering is minimal and can be considered negligible.

2. K-shell absorption jump factor

The K-shell absorption jump factor J_K can be experimentally determined using the following relationship (Akman et al. 2016b):

$$J_K = \sigma_{K\alpha}(E)[\sigma_t(E) - \sigma_{ts}(E)]^{-1}\omega_K^{-1}\left(1 + \frac{I_{K\beta}}{I_{K\alpha}}\right) \quad (1)$$

Where $\sigma_{K\alpha}$ is the K_α X-ray production cross section at photon energy E, σ_t is the total atomic absorption cross section which is determined using the transition geometry at photon energy E, σ_{ts} is the total (Compton and Coherent) atomic scattering cross section at photon energy E, ω_K is the K-shell fluorescence yield and $I_{K\beta}/I_{K\alpha}$ is the X-ray K_β to K_α intensity ratio.

On the other hand, the K-shell jump factor is defined as the probability that a K-shell electron is ejected during the photoelectric effect, as opposed to an electron from another shell or subshell. This parameter can be derived from the jump ratio using the following relation (Niranjana et al. 2013):

$$J_K = \frac{\tau_K}{\tau_K + \tau_L + \tau_M + \cdots\ldots\ldots + \sigma_{coh} + \sigma_{incoh}} = \frac{\sigma_a - \sigma_b}{\sigma_a} = \left[1 - \frac{1}{r_K}\right] \quad (2)$$

3. Davisson-Kirchner ratio

The K-shell Davisson-Kirchner ratio (DK_K) is defined as the ratio of the total photoelectric cross-section (σ_a) to the K-shell photoelectric cross-section at the K-edge. It provides insight into the relative contribution of higher-shell electrons to the photoelectric effect compared to that of K-shell electrons. This ratio can be derived from the K-shell jump factor, using the following relation (Hosur et al. 2011):

$$DK_K = \frac{\sigma_a}{\sigma_a - \sigma_b} = \frac{1}{J_K} \quad (4)$$

4. Oscillator strength

The K oscillator strength g_{K} represents the probability of electronic transitions from the K-shell to all allowed excited states. The theoretical method for its calculation was outlined by (James. 1948).

$$g_{\mathrm{K}} = \frac{m\, c\, E_{\mathrm{K}} \tau_{\mathrm{K}}}{2\pi^2 h^2 e^2 (n-1)} \quad . \tag{5}$$

Here n is the slope of the $\ln(\sigma_{\mathrm{PE}})$ versus $\ln(E)$ plot above the K-edge, m is the mass of the electron and E_{K} is the K-edge energy.

5. Data analysis

This study compiles experimental measurements of K-shell jump ratios and jump factors reported across a wide range of elements, spanning literature published from 1959 to 2023.

The database presented in this study integrates data from several authoritative compilations, including those by Budak et al. (2003), Polat et al. (2004), Akman et al. (2015), Sidhu et al. (2011), and Turhan et al. (2023), collectively contributing a total of 387 experimental values. To enhance the robustness and reliability of the dataset, these foundational sources are supplemented with carefully curated data extracted from additional peer-reviewed experimental studies. The resulting compilation serves as a comprehensive resource for analyzing the complexities of K-shell interactions and their dependence on atomic and environmental parameters.

- J_{K} A dataset of roughly 203 values, collected between 1996 and 2023, as shown in Fig. 1.a.
- r_{K} A dataset of roughly 184 values, collected between 1959 and 2021, as shown in Fig. 1.b.

III. Theoretical calculation

Theoretical calculations of X-ray absorption parameters are primarily performed using advanced computational frameworks and databases, such as the X-ray Cross Sections Database (XCOM) developed by the National Institute of Standards and Technology (NIST), and the Fundamental Parameters Approach (FPA), implemented in tools like FFAST. The XCOM database, based on the non-relativistic Hartree–Fock model, provides photon cross-sections for scattering, photoelectric absorption, and pair production, along with total attenuation coefficients for elements (Z = 1 to 100), compounds, and mixtures across a wide energy range (1 keV to 100 GeV). In contrast, the FFAST database offers high-precision measurements of X-ray mass attenuation coefficients using the X-ray extended-range technique. It includes detailed tabulations of atomic form factors, photoelectric absorption cross-sections, scattering cross-sections, and mass attenuation coefficients for elements with atomic numbers Z from 1 to 92 over an energy range from 1 eV to approximately 0.4 MeV. These resources are particularly critical for accurate calculations near absorption edges. To perform the calculations, the K-shell binding energy of the element of interest was first identified. Then, the mass attenuation coefficients at photon energies just below and just above the K-edge were retrieved from the XCOM and FFAST databases. These values were subsequently used to compute the jump factor and jump ratio using Eq.s (2) and (3), respectively. The resulting values are presented in Tables 2 and 3.

The accurate determination of the Davisson–Kirchner ratio and the oscillator strength requires precise photoelectric cross-section data at photon energies immediately above and below the absorption edge. To ensure accuracy and consistency, these cross-sectional values were sourced from the XCOM and FFAST databases. The theoretical basis for calculating the Davisson–Kirchner ratio is outlined in Eq. (4), which defines the fundamental relationship among the relevant physical parameters used in the analysis.

As shown in Eq. (5), the oscillator strength g_{K} can be accurately determined using three key variables: the K-edge energy E_{K}, the K-shell photoelectric cross-section τ_{K} at the absorption edge, and the slope parameter n. This methodology enables precise quantification of the oscillator strength, with the computational results systematically presented in Table 5.

IV. Semi-empirical calculation

Semi-empirical methods serve to bridge the gap between purely theoretical calculations and direct experimental measurements by integrating experimental data into theoretical models or by formulating empirical relationships grounded in established physical principles.

This method involves developing an analytical model for a specific K-shell absorption parameter (e.g., the K-shell jump ratio or jump factor) as a function of atomic number *Z*, using experimental data compiled from previously published literature, as shown in Fig. 1. To establish semi-empirical values for the K-shell absorption jump ratio and jump factor, a systematic approach was employed. For the K-shell absorption jump factor, a linear fit was applied to the weighted average experimental values $J_{\text{K-W}}(Z)$, reported by Daoudi et al. (2020) and Hamidani et al. (2023), as a function of atomic number *Z*. The resulting linear correlation is illustrated in Fig. 3(a).

$$J_{\mathrm{K-W}}(Z) = \sum_{\mathrm{i}=0}^{1} a_{\mathrm{iJ}} Z^{i} \tag{6}$$

Subsequently, the ratio between each experimental value and its corresponding weighted average value $R_{\mathrm{J}}(Z) = \frac{J_{\mathrm{k-exp}}}{J_{\mathrm{K-W}}}$ is calculated. These ratios are then plotted as a function of atomic number *Z*, and a second-order polynomial fit is applied to the resulting data. The fitted curve, which captures the trend in the variation of experimental deviations across atomic numbers, is presented in Fig. 4(a):

$$R_{\mathrm{J}}(Z) = \frac{J_{\mathrm{k-exp}}}{J_{\mathrm{K-W}}} = \sum_{\mathrm{i}=0}^{2} b_{\mathrm{iJ}} Z^{i} \tag{7}$$

Based on Eq.s (6) and (7), the semi-empirical expression for the K-shell absorption parameter can be formulated as follows:

$$(J_{\mathrm{K}})_{\mathrm{s-emp}} = J_{\mathrm{K-W}}(Z) \times R_{\mathrm{J}}(Z) \tag{8}$$

Secondly, for the K-shell absorption jump ratio, the weighted average values $r_{\mathrm{K-W}}(Z)$ derived from experimental data are modeled as a function of atomic number Z using a second-order polynomial fit. The resulting curve is shown in Fig. 3(b).

$$r_{\mathrm{K-W}}(Z) = \sum_{i=0}^{2} a_{\mathrm{ir}} Z^{i} \tag{9}$$

Thereafter, the same approach was applied to the K-shell absorption jump ratio. The ratio of each experimental value to its corresponding weighted average was calculated and plotted as a function of atomic number Z. A second-order polynomial fit was then applied to the data, and the resulting curve is presented in Fig. 4(b).

$$R_{\mathrm{r}}(Z) = \frac{r_{\mathrm{k-exp}}}{r_{\mathrm{K-W}}} = \sum_{\mathrm{i}=0}^{2} b_{\mathrm{ir}} Z^{i} \tag{10}$$

On the basis of Eq.s (9) and (10), the semi-empirical expression can be formulated as follows:

$$(r_{\mathrm{K}})_{\mathrm{s-emp}} = r_{\mathrm{K-W}}(Z) \times R_{\mathrm{r}}(Z) \tag{11}$$

The fitting coefficients a_{iJ}, b_{iJ} , a_{ir} and b_{ir} , corresponding to the jump factor, are presented in Table 1. A comprehensive summary of the semi-empirical calculations related to the jump ratios and jump factors is provided in Tables 2 and 3, respectively.

V. Empirical calculation

Empirical calculations play a vital role in advancing atomic physics, particularly in the accurate determination of key atomic parameters such as the K-shell absorption jump ratio and jump factor across a wide range of elements. Experimental investigations of these parameters often encounter considerable challenges (especially for heavy elements) due to their complex electronic configurations, which can hinder the precision of direct measurements. In contrast,

empirical methodologies offer robust frameworks for systematically analyzing such complexities. These approaches enable direct and reliable estimations, often surpassing the limitations of purely experimental techniques in capturing subtle electronic interactions. As a result, empirical models are essential for refining experimental data and enhancing predictive accuracy, particularly in cases where conventional experimental methods fall short in accounting for intricate interatomic dynamics. In the present study, a comprehensive statistical analysis of K-shell absorption characteristics is conducted using reported experimental data. Specifically, a linear regression is applied to model the K-shell absorption jump factor, while a second-order polynomial fit is used to describe the K-shell absorption jump ratio. Both parameters are examined as functions of atomic number to explore their systematic variation across different elements. The resulting curves are illustrated in Fig. 2.

$$(J_{\mathrm{K}})_{\mathrm{emp}} = -0.00203 \times Z + 0.94372 \tag{12}$$

$$(r_{\mathrm{K}})_{\mathrm{emp}} = 13.21758 - 0.18571 \times Z + 9.95724 \times 10^{-4} \times Z^2 \tag{13}$$

Tables 2 and 3 provide a comprehensive overview of the empirical calculations related to the K-shell absorption jump ratios and jump factors, respectively.

A semi-empirical method begins with a functional form that is informed by physical principles but is endowed with additional flexibility beyond strict first-principle estimates through the introduction of adjustable coefficients or empirical shape modifiers. This framework allows theoretical formulations to be refined by incorporating weighted averages of experimental data into analytical expressions, thereby preserving physical interpretability while enabling systematic extrapolations across atomic ranges. The principal limitation of this approach, however, lies in its dependence on the availability, quality, and consistency of experimental datasets, as inaccuracies in the latter can propagate into the derived functions.

By contrast, empirical methods are primarily data-driven. They do not invoke explicit theoretical constraints but instead rely on regression analyses or direct statistical modelling of

experimental results. Polynomial fitting provides a paradigmatic example of this strategy: a simple, and often arbitrary, mathematical form capable of representing variation is adjusted solely to follow the data. Such methods excel in reproducing experimental trends with robustness and practical accuracy within the measured domain. Nevertheless, their descriptive rather than explanatory nature limits their extrapolative power and restricts predictive reliability outside the calibrated range.

In summary, both semi-empirical and empirical methods reproduce experimental results with greater fidelity than purely theoretical calculations, yet they differ fundamentally in framework and predictive scope. While the semi-empirical approach maintains a closer link to physical laws and supports interpretability and generalisation, the empirical approach ensures straightforward applicability and robustness within the available dataset. Their complementary application provides a more comprehensive and reliable framework for evaluating K-shell absorption parameters.

The root-mean-square error ($\varepsilon_{\mathrm{rms}}$) is employed as a quantitative metric to assess the deviation between the calculated semi-empirical, empirical, and theoretical values of the jump ratios and jump factors and their corresponding experimental data. It is calculated using the following expression:

$$\varepsilon_{\mathrm{rms}} = \left[\frac{1}{N}\sum_{\mathrm{j}=1}^{\mathrm{N}}\left(\frac{\chi_{\mathrm{jexp}}-\chi_{\mathrm{jcalc}}}{\chi_{\mathrm{jcalc}}}\right)^{2}\right]^{\frac{1}{2}} \tag{14}$$

In this context, N represents the total number of experimental data points. The term χ_{exp} refers to the experimental jump ratios and corresponding jump factors, whereas χ_{calc} denotes the calculated values derived from both empirical and semi-empirical models.

The root-mean-square error ($\varepsilon_{\mathrm{rms}}$) values associated with the empirical, semi-empirical, and theoretical calculations are presented in Table 4 for each corresponding parameter. This metric

quantifies the extent to which the calculated jump ratios and jump factors align with experimental values. Lower $\varepsilon_{\mathrm{rms}}$ values indicate a closer agreement with experimental data, thereby enhancing the reliability of the results and reinforcing the validity of the models employed.

VI. Results and Discussion

This study presents a comprehensive evaluation of theoretical, semi-empirical, and empirical approaches used to determine key K-shell absorption parameters, specifically the jump ratio r_{K}, the absorption jump factor J_{K}, the Davisson-Kirchner ratio DK_{K}, and the oscillator strength g_{K}. The analysis included detailed comparisons between the values obtained through our calculations and those reported in the scientific literature, encompassing experimental measurements, established theoretical models (XCOM and FFAST), and other empirical or semi-empirical studies. To quantitatively assess the level of agreement, two statistical metrics are employed: the root-mean-square error $\varepsilon_{\mathrm{rms}}$ and the relative deviation (RD), defined as $\mathrm{RD}(\%) = \left|\left(\chi_{\mathrm{exp}} - \chi_{\mathrm{calc}}\right)/\chi_{\mathrm{calc}}\right| \times 100$. These metrics provide a rigorous basis for evaluating the degree of concordance between the calculated and experimental values. This thorough assessment highlights the strengths and limitations of each approach in accurately characterizing these fundamental atomic parameters.

- **K-shell Absorption Jump Factor**

The semi-empirical calculations for the K-shell absorption jump factor J_{K} exhibit strong agreement with experimental data across the atomic number range $22 \leq Z \leq 92$. As illustrated in Fig. 5(a), the trends predicted by the semi-empirical model closely align with experimental values and independently fitted data reported by various authoritative sources (e.g., Kaçal, 2015a; Kaya 2008b; Budak, 2003; Turhan, 2023). A detailed quantitative comparison of these results is presented in Table 2. Notably, the root-mean-square error $\varepsilon_{\mathrm{rms}}$ for the semi-empirical

J_K values is remarkably low, with an overall $\varepsilon_{\mathrm{rms}}$ of 1.87% (Table 4), indicating a high level of accuracy for this approach. This performance notably exceeds that of the purely theoretical predictions provided by the XCOM (3.90%) and FFAST (3.46%) databases. The empirical model also shows strong agreement with experimental data, achieving an overall $\varepsilon_{\mathrm{rms}}$ of 1.84% (Table 4), further demonstrating its effectiveness in capturing the general experimental trends.

A more detailed examination of the elemental breakdown, as illustrated in Fig. 6, reveals that the root-mean-square error $\varepsilon_{\mathrm{rms}}$ values for the semi-empirical J_K generally remain below 2% for most elements. Notably, exceptionally low deviations are observed, such as 0.12% for technetium (Z = 43). Similarly, the empirical $\varepsilon_{\mathrm{rms}}$ values frequently fall within a comparable low range, for example, 0.54% for vanadium (Z = 23). However, it is important to acknowledge certain elements that exhibit noticeably higher deviations across all approaches. For instance, in the case of uranium (Z = 92), the semi-empirical $\varepsilon_{\mathrm{rms}}$ is 3.97% (with a relative deviation, RD, of 3.97%), the empirical value is 3.33% (RD = 3.33%). In comparison, the theoretical models show significantly larger deviations 9.61% for XCOM and 8.40% for FFAST. A similar pattern is observed for iridium (Z = 77), where the semi-empirical RD is 2.44% and the empirical RD is 1.64%, whereas XCOM and FFAST show deviations of 5.33% and 5.41%, respectively. These larger discrepancies can often be attributed to the heterogeneity of experimental conditions and the methodological differences among the various studies from which the data were compiled. In addition, relativistic effects (particularly relevant for high-Z elements) introduce further complexity that may result in divergence between theoretical predictions and experimental measurements. Despite these isolated instances of elevated deviation, the overall consistency and low $\varepsilon_{\mathrm{rms}}$ values observed for the semi-empirical J_{K}, closely followed by the empirical results, reaffirm the robustness and enhanced predictive capability of these approaches when compared to purely theoretical databases in this comprehensive evaluation.

- **K-shell Absorption Jump Ratio**

In parallel, the K-shell absorption jump ratio r_{K} values derived from the semi-empirical approach demonstrate strong agreement with existing experimental data. This correlation is visually confirmed in Fig. 5(b), where the semi-empirical curve closely follows the trends reported by various studies (e.g., Kaçal 2015a; Kaya 2008b; Veigele, 1973). Detailed quantitative comparisons are provided in Table 3. The overall root-mean-square error $\varepsilon_{\mathrm{rms}}$ for the semi-empirical r_{K} values is 6.54% (Table 4), indicating a substantially better alignment with experimental results compared to the theoretical predictions from the XCOM (21.98%) and FFAST (17.85%) databases, both of which exhibit significantly higher deviations. The empirical approach also performs well, with an overall $\varepsilon_{\mathrm{rms}}$ of 8.21% (Table 4), demonstrating its capability to capture the general behavior of the r_K parameter effectively.

A more detailed analysis of the element-specific root-mean-square error $\varepsilon_{\mathrm{rms}}$ for the K-shell absorption jump ratio r_{K}, reveals varying levels of agreement across different methodologies, as illustrated in Fig. 7. While many elements exhibit very low deviations for the semi-empirical model, such as 0.12% for erbium (Z = 68), specific atomic ranges, particularly among lower-Z elements, show more pronounced discrepancies across all approaches. For example, in the case of nickel (Z = 28), the semi-empirical $\varepsilon_{\mathrm{rms}}$ value is 13.33% (with a relative deviation, RD, of 17.65%), and the empirical value is 14.43% (RD = 12.34%). In comparison, the theoretical models show significantly higher deviations 21.20% for XCOM and 17.32% for FFAST. A similar pattern is observed for silver (Z = 47), with the semi-empirical RD at 17.13%, empirical at 21.44%, and much larger deviations from XCOM (39.61%) and FFAST (37.33%). These elevated deviations, similar to those observed for the jump factor J_{K}, may arise from inherent challenges in precisely measuring absorption parameters for specific elements or under experimental conditions where subtle interatomic effects become increasingly influential. Despite these localized discrepancies, the overall consistency of the trends and the significantly

lower $\varepsilon_{\mathrm{rms}}$ values obtained from the semi-empirical and empirical formulations, particularly when compared to purely theoretical models, underscores the enhanced reliability and predictive capability of these approaches for r_{K} within the context of this comprehensive evaluation.

- **Davisson-Kirchner Ratio and Oscillator Strength**

Theoretical calculations for the K-shell Davisson–Kirchner ratio $\mathrm{DK_K}$ and oscillator strength g_{K}, derived using data obtained from the well-established XCOM and FFAST databases (Table 5), provide a reliable theoretical baseline for these parameters. Comparisons with available fitted and experimental values, such as those reported by Hubbell (1996), Mallikarjuna et al. (2002), and Puttaswamy et al. (1981), generally demonstrate good agreement across the studied range of atomic numbers. The systematic trends exhibited by the $\mathrm{DK_K}$ and g_{K} values as functions of atomic number Z are in full accordance with established physical principles, accurately reflecting the nuanced variations in electronic structure and X-ray interaction probabilities observed across the periodic table.

The rigorous application of a consistent methodology for extracting photoelectric cross-section data from established databases ensures both the internal coherence and the inherent reliability of the calculated $\mathrm{DK_K}$ and g_{K} values. Although direct experimental comparisons across all elements for these specific parameters remain limited due to data availability, the observed consistency with published literature further supports the validity of the theoretical framework and confirms the appropriateness of the selected data sources.

As an extension of the present study, the K-shell absorption parameters, including the jump factor J_{K}, the jump ratio r_{K}, the oscillator strength g_{K}, and the Davisson–Kirchner ratio $\mathrm{DK_K}$, have been estimated for elements in the range $Z = 93$ to 100. Given that reliable experimental data are available only up to $Z = 92$, the values for $Z > 92$ were obtained through extrapolation

of the empirical and semi-empirical relations developed in this work. These models were originally constructed by fitting to data within the experimentally accessible range (Z = 22–92) and are here extended beyond this limit under the assumption that the established trends continue smoothly. Theoretical values for this range were derived solely using the XCOM database, since FFAST provides data only up to Z = 92.

The extrapolated results, summarized in Table 6, are of potential relevance to nuclear science applications. X-ray transmission techniques are commonly used to determine concentrations of actinides in aqueous solutions of irradiated nuclear fuel. While the primary focus is often on major actinides, such as uranium and plutonium, there is increasing interest in minor actinides, including americium and curium, particularly in the context of advanced nuclear fuel cycles and waste characterization. Although the precision of available step-height data at these energies remains limited (and thus unsuitable for direct quantitative analysis, which currently relies on the use of representative physical standards) Croft et al., (2015), such parameters can support modeling efforts and serve as a theoretical baseline for future experimental validation. In practice, analytical instruments, such as the Hybrid K-Edge Densitometer (HKRD) used in nuclear safeguards to provide accountancy tank concentrations of (U) and (Pu) McElroy et al., (2015a; 2015b), are typically calibrated using chemically prepared solution standards, rather than relying solely on absorption step measurements.

VII. Conclusion

This work presents a comprehensive and novel evaluation of K-shell absorption parameters, including the absorption jump ratio r_K, the jump factor J_K, the Davisson–Kirchner ratio DK_K, and the oscillator strength g_K) Through meticulous compilation and critical analysis of experimental data from a broad range of sources, combined with the use of established theoretical databases (XCOM and FFAST), new semi-empirical and empirical formulations for

J_K and r_K. have been developed and validated. These formulations span a wide range of elements, covering atomic numbers from $Z = 22$ to 100 for J_K and $Z = 18$ to 100 for r_K.

Our findings demonstrate that the proposed theoretical, semi-empirical, and empirical models generally exhibit excellent agreement with existing experimental data and established predictions. Quantitative assessment, particularly through the systematic application of root-mean-square error ε_{rms} and relative deviation RD, confirms the comparative accuracy of the different approaches. The semi-empirical models offer superior accuracy for both J_K and r_K, outperforming direct theoretical calculations from XCOM and FFAST, which often show larger deviations. The empirical methods also prove highly effective, capturing systematic trends and achieving competitive accuracy across many elements.

These results underscore the effectiveness and precision of applying diverse methodological strategies to obtain reliable estimations of critical atomic parameters. Beyond supplementing existing literature, the values derived for K-shell absorption parameters, via theoretical, semi-empirical, and empirical methods, constitute an updated and valuable resource for the broader scientific and technical community. Their integration into comprehensive atomic databases will enhance the accuracy of simulations and analytical applications in various disciplines, including X-ray spectroscopy, materials science, radiation dosimetry, and medical physics.

Moreover, this work makes a significant contribution to the refinement of atomic interaction models by deepening the understanding of fundamental K-shell absorption mechanisms. It reinforces the ongoing need for precise parameterization in advancing the field of X-ray physics. Although some element-specific discrepancies are acknowledged, these primarily indicate opportunities for future experimental research aimed at reducing data heterogeneity and further improving the accuracy of predictive models.

VIII. Acknowledgments

We gratefully acknowledge the support of the DGRSDT, Ministry of Higher Education and Scientific Research, Algeria. This work was done with the support of Mohamed El Bachir El Ibrahimi University, under project (PRFU) Nº: B00L02UN340120230004. This work was also supported by the Fundação para a Ciência e Tecnologia (FCT), Portugal through contracts UIDP/50007/2020 (LIP) and UID/FIS/04559/2020 (LIBPhys). S.C. warmly acknowledges the financial support of Lancaster University, and A.F. gratefully acknowledges the support of the Joint Research Centre of the European Commission.

Figure captions:

Fig. 1. (a) The distribution of J_{K-EXP} for each reference from which the databases are extracted according to the atomic number Z (from 1996 to 2023). ●: (Ayala and Mainardi. 1996); ●: (Chantler *et al*., 2001); ●: (Ertugrul *et al*., 2002); ●: (Mallikarjuna *et al.,* 2002); ◆: (Budak *et al.,* 2003); ○: (Polat *et al.,* 2004); ○: (Budak and Polat. 2004); ○: (Polat *et al.,* 2005); ○: (Nayak and Badiger. 2006); ⊖: (Bennal and Badiger. 2007); ⊖: (Kaya *et al.,* 2007); ⊖: (Kaya *et al.,* 2008b); ⊖: (Rae *et al.,* 2010); ▲: (Sidhu *et al.,* 2011); ▲: (Hosur *et al.,* 2011); ▲: (Kaya *et al.,* 2011); ▲: (Niranjana *et al.,* 2013); ▲: (Polat *et al.,* 2013); △: (Kaçal *et al.,* 2015a); △: (Kaçal *et al.,* 2015b); △: (Akman *et al.,* 2015); ⧋: (Niranjana and Badiger. 2015); ⧋: (Küçükönder and Topuz. 2016); ⧋: (Akman *et al.,* 2016a); ⧋: (Akman *et al.,* 2016b); ⧋: (Küçükönder *et al.,* 2017); ■: (Anand *et al.,* 2018); ■: (Turhan *et al.,* 2018); ■: (Turşucu. 2019); ▼: (Ekanayake *et al.,* 2021); ▶: (Turhan and Akman. 2023).

(b) The distribution of r_{K-EXP} for each reference from which the databases are extracted according to the atomic number Z (from 1983 to 2021). ◆: (Hopkins.1959); ◆: (Deslattes *et al.,* 1983); ◆:(Scofield. 1974); ⬢ :(Puttaswamy *et al.,* 1981); ⬢ :(Rao *et al.,* 1984); ○ :(Deutscht and Hart. 1986); ○:(Lingam *et al.,* 1989); ●: (Ayala and Mainardi. 1996); ●: (Chantler *et al*., 2001); ●: (Ertugrul *et al*., 2002); ●: (Mallikarjuna *et al.,* 2002);○: (Polat *et al.,* 2004); ○: (Budak and Polat. 2004); ○: (Nayak and Badiger. 2006); ⊖: (Kaya *et al.,* 2007); ⊖: (Kaya *et al.,* 2008b); ⊖: (Rae *et al.,* 2010); ▲: (Sidhu *et al.,* 2011); ▲: (Hosur *et al.,* 2011); ▲: (Kaya *et al.,* 2011); ▲: (Niranjana *et al.,* 2013); ▲: (Polat *et al.,* 2013); △: (Kaçal *et al.,* 2015a); △: (Kaçal *et al.,* 2015b); △: (Akman *et al.,* 2015); ⧋: (Niranjana and Badiger. 2015); ⧋: (Küçükönder and Topuz. 2016); ⧋: (Akman *et al.,* 2016a); ⧋: (Küçükönder *et al.,* 2017); ■: (Anand *et al.,* 2018); ■: (Turhan *et al.,* 2018); ■: (Turşucu. 2019); ▼: (Ekanayake *et al.,* 2021).

Fig. 2. Distribution of the experimental as a function of the atomic number Z.

(a) Jump factor $J_{\mathrm{k-exp}}$ values the curve is the fitting according to Eq. (12)

(b) Jump ratio $r_{\mathrm{k-exp}}$ values the curve is the fitting according to Eq. (13)

Fig.3. Distribution of weighted (w) values as a function of the atomic number Z.

(a) The weighted of jump factor $J_{\mathrm{k-w}}$ values the curve is the fitting according to Eq. (6)

(b) The weighted of jump ratio $r_{\mathrm{k-w}}$ values the curve is the fitting according to Eq. (9)

Fig.4. Distribution of proportional (R) values as a function of the atomic number Z.

(a) The proportional of jump factor $R_{\mathrm{J}}(Z) = \frac{J_{\mathrm{k-exp}}}{J_{\mathrm{K-W}}}$ values the curve is the fitting according to Eq. (7)

(b) The proportional of jump ratio $R_{\mathrm{r}}(Z) = \frac{r_{\mathrm{k-exp}}}{r_{\mathrm{K-W}}}$ values the curve is the fitting according to Eq. (10)

Fig. 5. Comparison of present empirical, semi-empirical, and theoretical with experimental values for as a function of atomic number Z.

(a) For jump factor (J_K) values

(b) For jump ratio (r_K) values

Fig. 6. For jump factor (J_K) values; the root-mean-square error ($\varepsilon_{rms}\%$) for each element is evaluated for the present empirical, semi-empirical, and theoretical (XCOM and FFAST) as a function of the atomic number *Z*.

Fig. 7. For jump ratio (r_K) values; the root-mean-square error ($\varepsilon_{rms}\%$) for each element is evaluated for the present empirical, semi-empirical, and theoretical (XCOM and FFAST) as a function of the atomic number *Z*.

References

Ade, H., & Hitchcock, A. P. (2008). NEXAFS microscopy and resonant scattering: Composition and orientation probed in real and reciprocal space. Polymer, 49(3), 643-675.

Akman, F., Kaçal, M. R., & Durak, R. (2016a). Chemical effect on the K shell absorption parameters of some selected cerium compounds. Journal of Instrumentation, 11(08), P08006.

Akman, F., Kaçal, M. R., & Durak, R. (2016b). The excitation probabilities of Kα, β and Lα1, 2 for some elements in $56 \leq Z \leq 68$ at 59.54 keV. Radiation Physics and Chemistry, 119, 29-36.

Akman, F., Durak, R., Kaçal, M. R., Turhan, M. F., & Akdemir, F. (2015a). Determination of K-shell absorption jump factors and jump ratios for La_2O_3, Ce and Gd using two different methods. Radiation Physics and Chemistry, 107, 75-81.

Akman, F., Durak, R., & Kaçal, M. R. (2015b). Determination of K shell absorption parameters for some lanthanides using the X-ray attenuation method. Canadian Journal of Physics, 93(12), 1532-1540.

Akman, F., Durak, R., Kaçal, M. R., & Bezgin, F. (2016). Study of absorption parameters around the K edge for selected compounds of Gd. X-Ray Spectrometry, 45(2), 103-110.

Amari, K., Kahoul, A., Sampaio, J. M., Kasri, Y., Marques, J. P., Parente, F., ... & Berkani, B. (2024). Empirical calculation of K-shell fluorescence cross sections for elements in the atomic range $16 \leq Z \leq 92$ by photon effects ranging from 5.46 to 123.6 keV (Three-dimensional formulae). Physica Scripta, 99(10), 105402.

Anand, L., Gudennavar, S. B., Bubbly, S. G., Kerur, B. R., & Horakeri, L. D. (2018, August). K-shell jump ratio and jump factor of 3d elements. In AIP Conference Proceedings (Vol. 1994, No. 1). AIP Publishing.

Ayala, A. P., & Mainardi, R. T. (1996). Measurement of the K X-ray absorption jump ratio of erbium by attenuation of a Compton peak. Radiation Physics and Chemistry, 47(2), 177-181.

Bennal, A. S., & Badiger, N. M. (2007). Measurement of K shell absorption and fluorescence parameters for the elements Mo, Ag, Cd, In and Sn using a weak gamma source. Journal of Physics B: Atomic, Molecular and Optical Physics, 40(11), 2189.

Berger, M. J., Hubbell, J. H., Seltzer, S. M., Chang, J., Coursey, J. S., Sukumar, R., Zucker, D. S., & Olsen, K. (2010). *XCOM: Photon Cross Section Database* (Version 1.5) [Online]. National Institute of Standards and Technology. https://physics.nist.gov/xcom

Berkani, B., Kahoul, A., Sampaio, J. M., Daoudi, S., Marques, J. P., Parente, F., ... & Amari, K. (2025a). Semi-empirical calculation of K to Li sub-shell, K to L, and M shell vacancy transfer probability for elements in the atomic range $16 \leq Z \leq 92$. Nuclear Instruments and Methods in Physics Research Section B: Beam Interactions With Materials and Atoms, 563, 165689.

Berkani, B., Kahoul, A., Sampaio, J. M., Daoudi, S., Marques, J. P., Parente, F., ... & Amari, K. (2025b). Relativistic and semi-theoretical calculations of K-shell to L-shell/subshell vacancy transfer probabilities. Spectrochimica Acta Part B: Atomic Spectroscopy, 224, 107089.

Budak, G., Karabulut, A., & Ertuğrul, M. (2003). Determination of K-shell absorption jump factor for some elements using EDXRF Technique. Radiation Measurements, 37(2), 103-107.

Budak, G., & Polat, R. E. C. E. P. (2004). Measurement of the K X-ray absorption jump factors and jump ratios of Gd, Dy, Ho and Er by attenuation of a Compton peak. Journal of Quantitative Spectroscopy and Radiative Transfer, 88(4), 525-532.

Broll, N. (1986). Quantitative x-ray fluorescence analysis. Theory and practice of the fundamental coefficient method. X-Ray Spectrometry, 15(4), 271-285.

Cengiz, E., Aylıkcı, V., Kaya, N., Apaydın, G., Tıraşoğlu, E., 2008. Chemical effects on K and L shell production cross sections and transfer probabilities in Nb compounds. J Radioanal Nucl Chem 278, 89–96.

Chantler, C. T. (1995). Theoretical form factor, attenuation, and scattering tabulation for Z = 1–92 from E = 1–10 eV to E = 0.4–1.0 MeV. Journal of Physical and Chemical Reference Data, 24(1), 71–643.

Chantler, C. T., Olsen, K., Dragoset, R. A., Chang, J., Kishore, A. R., Kotochigova, S. A., & Zucker, D. S. (2005). X-Ray Form Factor, Attenuation and Scattering Tables (Version 2.1) [Online]. National Institute of Standards and Technology. https://physics.nist.gov/ffast

Croft, S., Nicholson, A. D., & McElroy, R. D. (2015). Mass Attenuation Coefficient Data for Hybrid K-Edge Densitometry. Oak Ridge National Lab.(ORNL), Oak Ridge, TN (United States).

Cromer, D. T. (1965). Anomalous dispersion corrections computed from self-consistent field relativistic Dirac–Slater wave functions. Acta Crystallographica, 18(1), 17-23.

Daoudi, S., Kahoul, A., Kup Aylikci, N., Sampaio, J.M., Marques, J.P., Aylikci, V., Sahnoune, Y., Kasri, Y., Deghfel, B., 2020. Review of experimental photon-induced K β /K α intensity ratios. Atomic Data and Nuclear Data Tables 132, 101308.

Ekanayake, R. S., Chantler, C. T., Sier, D., Schalken, M. J., Illig, A. J., de Jonge, M. D., ... & Tran, C. Q. (2021). High-accuracy measurement of mass attenuation coefficients and the imaginary component of the atomic form factor of zinc from 8.51 keV to 11.59 keV, and X-ray absorption fine structure with investigation of zinc theory and nanostructure. Journal of Synchrotron Radiation, 28(5), 1492-1503.

Ertugrul, M., Karabulut, A., & Budak, G. (2002). Measurement of the K shell absorption jump factor of some elements. Radiation Physics and Chemistry, 64(1), 1-3.

Hamidani, A., Daoudi, S., Kahoul, A., Sampaio, J.M., Marques, J.P., Parente, F., Croft, S., Favalli, A., Kup Aylikci, N., Aylikci, V., Kasri, Y., & Meddouh, K. (2023). "Updated database, semi-empirical and theoretical calculation of Kβ⁄Kα intensity ratios for elements ranging from $_{11}$Na to $_{96}$Cm". At. Data Nucl. Data Tables 149, 101549–58.

Hopkins, J. I. (1959). Low-Energy X-Ray Attenuation Measurements for Elements of Low Atomic Number. Journal of Applied Physics, 30(2), 185-187.

Hosur, S. B., Badiger, N. M., & Naik, L. R. (2008). Determination of the K shell oscillator strengths and the imaginary form factors of atoms using a weak beta source. Journal of Physics B: Atomic, Molecular and Optical Physics, 41(9), 095003.

Hosur, S. B., Naik, L. R., & Badiger, N. M. (2011). Study of the K shell photoelectric parameters of Dy, Yb and W atoms using low energy bremsstrahlung radiation. The European Physical Journal D, 62, 155-161.

Hubbell, J. H., & Seltzer, S. M. (1996). Tables of X-ray mass attenuation coefficients and mass energy-absorption coefficients from 1 keV to 20 MeV for elements *Z* = 1 to 92 and 48 additional substances of dosimetric interest (NISTIR 5632). National Institute of Standards and Technology.

James, R. W. (1948). *The optical principles of diffraction of X-rays* (Chapter IV). London: Bell & Sons.

Kacal, M. R., Han, İ., & Akman, F. (2015a). Measurements of K shell absorption jump factors and jump ratios using EDXRF technique. The European Physical Journal D, 69, 103.

Kaçal, M. R., Han, İ., & Akman, F. (2015b). Determination of K shell absorption jump factors and jump ratios of 3d transition metals by measuring K shell fluorescence parameters. Applied Radiation and Isotopes, 95, 193-199.

Kahoul, A., Aylikci, V., Deghfel, B., Aylikci, N. K., & Nekkab, M. (2014). New empirical formulae for calculation of average M-shell fluorescence yields. Journal of Quantitative Spectroscopy and Radiative Transfer, 145, 205-213.

Kaya, N., Tıraşoğlu, E., Apaydın, G., Aylıkcı, V., & Cengiz, E. (2007). K-shell absorption jump factors and jump ratios in elements between Tm (Z= 69) and Os (Z= 76) derived from new mass attenuation coefficient measurements. Nuclear Instruments and Methods in Physics Research Section B: Beam Interactions with Materials and Atoms, 262(1), 16-23.

Kaya, N. E. C. A. T. İ., Apaydın, G., Aylıkcı, V., Cengiz, E., & Tıraşoğlu, E. (2008a). K shell, L shell–subshell and M shell–subshell photoeffect cross-sections in elements between Tb (Z= 65) and U (Z= 92) at 123.6 keV. Radiation Physics and Chemistry, 77(2), 101-106.

Kaya, N., Tıraşoğlu, E., Apaydın, G. (2008b). Determination of K shell absorption jump factors and jump ratios in the elements between Tm (Z = 69) and Os (Z = 76) by measuring K shell fluorescence parameters. Nuclear Instruments and Methods in Physics Research B 266,1043–1048.

Kaya, N. E. C. A. T. İ., Apaydin, G. Ö. K. H. A. N., & Tirasoglu, E. (2011). Measurement of K-shell jump ratios and jump factors for some elements in $76 \leq Z \leq 92$ using EDXRF spectrometer. Radiation Physics and Chemistry, 80(6), 677-681.

Koningsberger, D. C., & Prins, R. (Eds.). (1988). X-ray absorption: Principles, applications, techniques of EXAFS, SEXAFS and XANES. Wiley.

Küçükönder, A., & Topuz, H. (2016). Determination of K shell absorption jump factors for As, Se, Sr, Ag, Ba, La and Ce compounds. In AIP Conference Proceedings (Vol. 1722, No. 1). AIP Publishing.

Küçükönder, A., & Saka, E. K. (2017). Chemical effects on K shell absorption jump factors and jump ratios of 3d transition metal compounds. Canadian Journal of Physics, 95(6), 600-604.

Gupta, M. K., Singh, G., Dhaliwal, A. S., & Kahlon, K. S. (2015). Measurement of absorption edge parameters near K edge for the compounds of Zn, Zr, Cd, Ba and Pb. Journal of Alloys and Compounds, 623, 407-412.

Lingam, S. C., Babu, K. S., Kumar, V. P., & Reddy, D. K. (1989). Total-to-K-shell photoelectric cross-section ratios in some rare-earth and high-Z elements. Canadian Journal of Physics, 67(2-3), 139-142.

Mallikarjuna, M. L., Gowda, S. A., Krishnaveni, S., Gowda, R., & Umesh, T. K. (2002). Studies on photon interaction around the K-edge of some elements. Nuclear Science and Engineering, 140(1), 96-102.

McElroy, R. D., Cleveland, S. L., Croft, S., Mickum, G. S., & Nicholson, A. D. (2015a). Relative Actinide K-Shell Vacancy Production Rates in Hybrid K-Edge Densitometry. Oak Ridge National Lab.(ORNL), Oak Ridge, TN (United States).

McElroy, R. D., Croft, S., Mickum, G. S., & Cleveland, S. L. (2015b). Spectral fitting approach to the hybrid K-edge densitometer: preliminary performance results. Oak Ridge National Lab.(ORNL), Oak Ridge, TN (United States).

Meddouh, K., Daoudi, S., Kahoul, A., Sampaio, J. M., Marques, J. P., Parente, F., ... & Hamidani, A. (2023). Average K, L, and M-shell fluorescence yields: A new semi-empirical formulae. Radiation Physics and Chemistry, 202, 110481.

Nayak, S. V., & Badiger, N. M. (2006). A novel method for measuring K-shell photoelectric parameters of high-*Z* elements. Journal of Physics B: Atomic, Molecular and Optical Physics, 39(12), 2893.

Niranjana, K. M., Krishnananda, Badiger, N. M., Joseph, D., & Kailas, S. (2013). Determination of K shell parameters of silver using high resolution HPGe detector spectrometer. International Journal of Nuclear Energy Science and Technology, 7(3), 179-190.

Niranjana, K. M., & Badiger, N. M. (2015). K shell parameters of some lanthanide elements using bremsstrahlung. Radiation Physics and Chemistry, 107, 59-64.

Poehn, C., Wernisch, J., & Hanke, W. (1985). Least-squares fits of fundamental parameters for quantitative x-ray analysis as a function of Z ($11 \leq Z \leq 83$) and E (1 keV$\leq$ E$\leq$ 50 keV). X-ray Spectrometry, 14(3), 120-124.

Polat, R., İçelli, O., & Budak, G. (2004). New method to measure the K-shell absorption jump factor in some rare-earth elements. Analytica chimica acta, 505(2), 307-314.

Polat, R. E. C. E. P., Budak, G., Gürol, A., Karabulut, A., & Ertugrul, M. (2005). K-shell absorption jump factors for the elements Ag, Cs, Ba and La derived from new mass attenuation coefficient measurements using EDXRF technique. Radiation measurements, 39(4), 409-415.

Polat, R., İçelli, O., Yalçın, Z., Pesen, E., & Orak, S. (2013). Measurement of K-shell absorption jump factors and jump ratios in some lanthanide elements using EDXRF technique. Annals of Nuclear Energy, 54, 267-273.

Puttaswamy, K. S., Gowda, R., & Sanjeevaiah, B. (1981). Total and K-shell photoeffect cross sections at K-edges of Cu, Zr, Ag, Sn, Ta, Au, and Pb. Canadian Journal of Physics, 59(7), 853-858.

Rao, G. K., Perumallu, A., & Rao, A. N. (1984). A study on atomic photo effect cross sections at the K-edge in high *Z*-elements. Physica B+ C, 125(3), 334-340.

Rindfleisch. H. Ann. der Phys. 1937. 28. 409. - Annalen der Physik journal. volume 28. page 409.

Sahnoune, Y., Kahoul, A., Kasri, Y., Deghfel, B., Medjadi, D. E., Khalfallah, F., Daoudi, S., Aylikçi, V., Küp Aylikçi, N., & Nekkab, M. (2016). L_1, L_2, and L_3 subshell fluorescence yields: Updated database and new empirical values". Radiat. Phys. Chem. 125, 227-251.

Scofield, J. H. (1973). Theoretical photoionization cross sections from 1 to 1500 keV (UCRL-51326). Lawrence Livermore Laboratory, University of California.

Sidhu, B. S., Dhaliwal, A. S., Mann, K. S., & Kahlon, K. S. (2011). Measurement of K-shell absorption edge jump factors and jump ratios of some medium Z elements using EDXRF technique. Radiation Physics and Chemistry, 80(1), 28-32.

Stöhr, J. (1992). *NEXAFS Spectroscopy*. Springer Series in Surface Sciences. Springer.

Stöhr, J., & Outka, D. A. (1987). Determination of molecular orientations on surfaces from the angular dependence of near-edge X-ray-absorption fine-structure spectra. *Physical Review B*, *36*(15), 7891.

Turhan, M. F., Durak, R., Akman, F., Kaçal, M. R., & Araz, A. (2018). Determination of some selected absorption parameters for Cd, La and Ce elements. Radiation Physics and Chemistry, 156, 101-108.

Turhan, M. F., & Akman, F. (2023). K shell fluorescence parameters of some elements at 59.54 keV: Experimental and theoretical results. Nuclear Instruments and Methods in Physics Research Section B: Beam Interactions with Materials and Atoms, 534, 16-25.

Turşucu, A. (2019). K shell absorption jump ratios and jump factor measurements for some elements in the range of $40 \leq Z \leq 50$. Canadian Journal of Physics, 97(7), 786-790.

Veigele, W. J. (1973). Photon cross sections from 0.1 keV to 1 MeV for elements *Z*= 1 to *Z*= 94. Atomic Data and Nuclear Data Tables, 5(1), 51-111.

Zidi, A., Kahoul, A., Marques, J. P., Daoudi, S., Sampaio, J. M., Parente, F., ... & Berkani, B. (2024). Investigating empirical and theoretical calculations for intensity ratios of L-Shell X-ray transitions in atoms with 39≤ Z≤ 94. Journal of Electron Spectroscopy and Related Phenomena, 275, 147473.

Zidi, A., Kahoul, A., Marques, J. P., Amari, K., Daoudi, S., Sampaio, J. M., ... & Berkani, B. (2025). Intensity ratios of ILβ/ILα and ILγ/ILα: Semi-theoretical formulae for diverse elements under photon excitation with 1.9 keV< E_{inc}≤ 200 keV. Nuclear Instruments and Methods in Physics Research Section A: Accelerators, Spectrometers, Detectors and Associated Equipment, 1075, 170416.

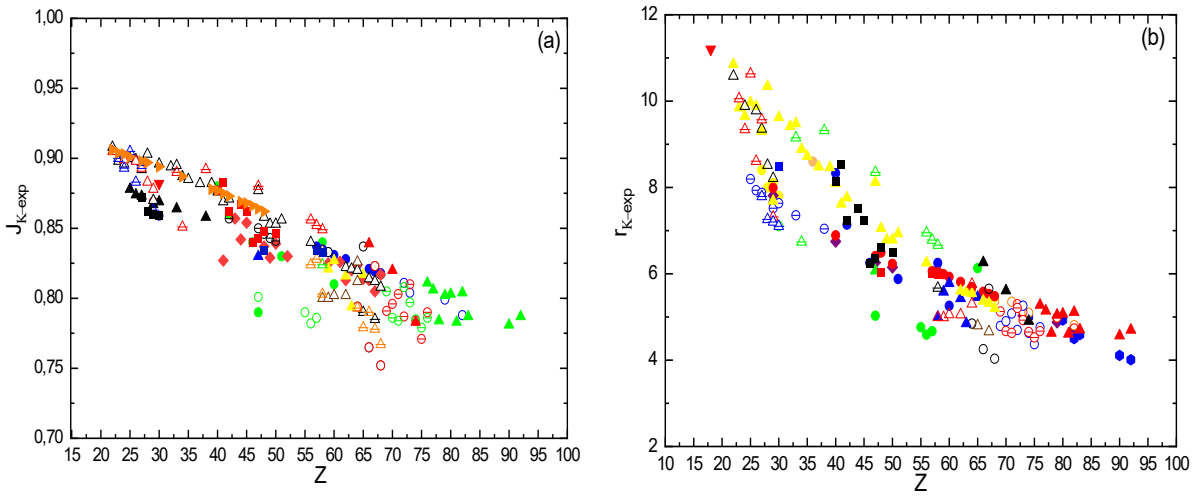

Fig. 1

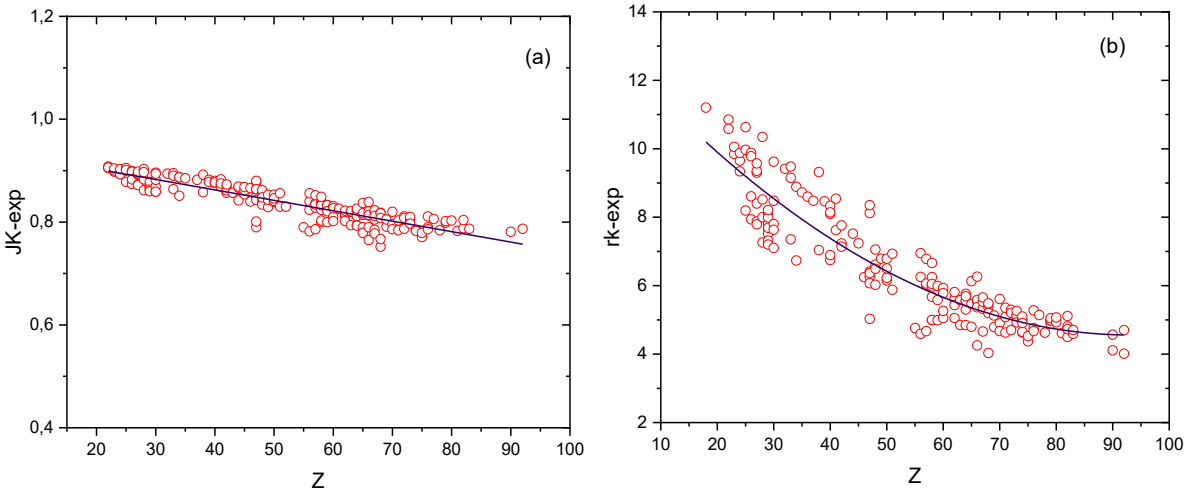

Fig. 2

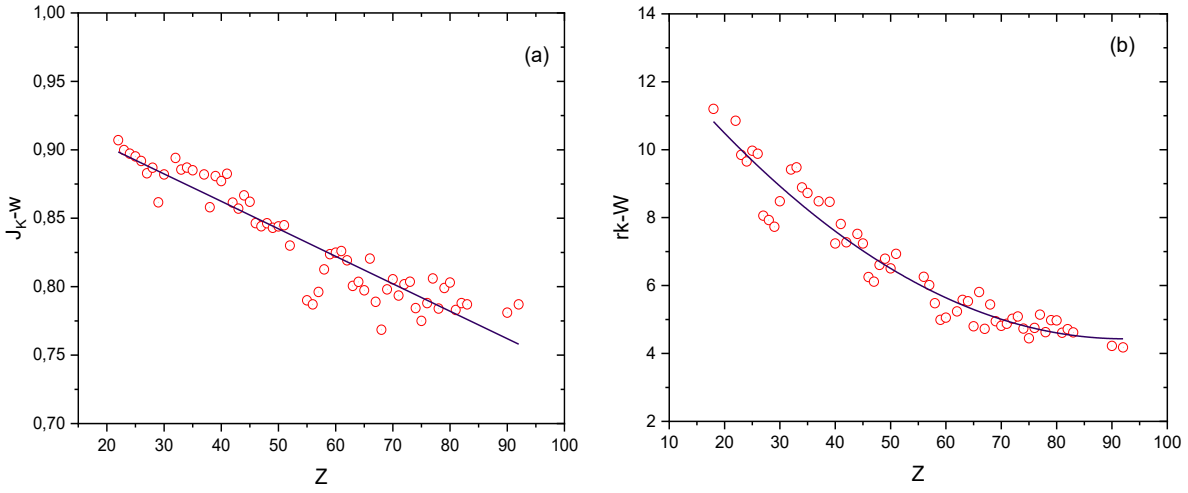

Fig.3

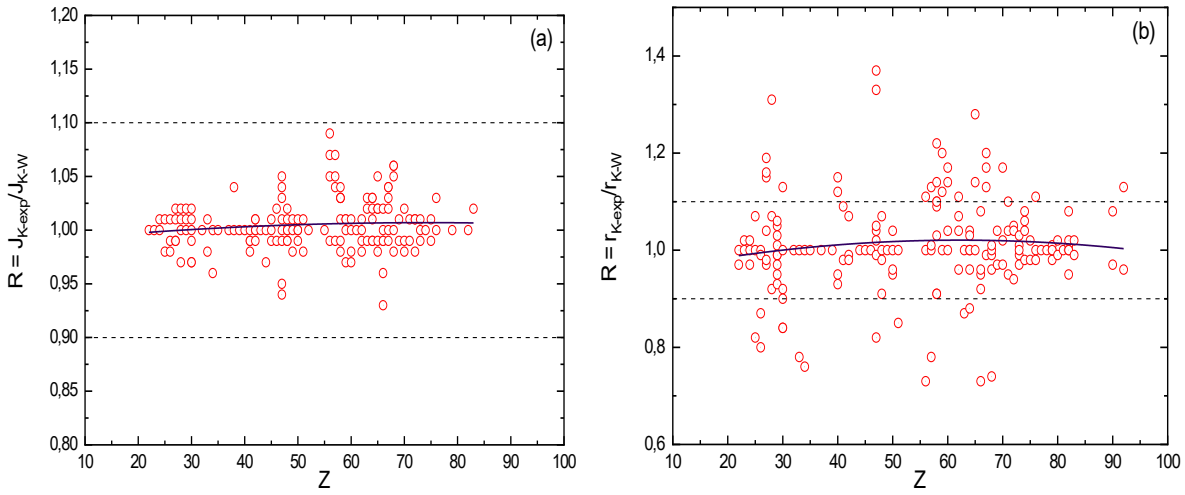
(a)
R = J_K-exp/J_K-W
Z
(b)
R = r_K-exp/r_K-W
Z

Fig.4

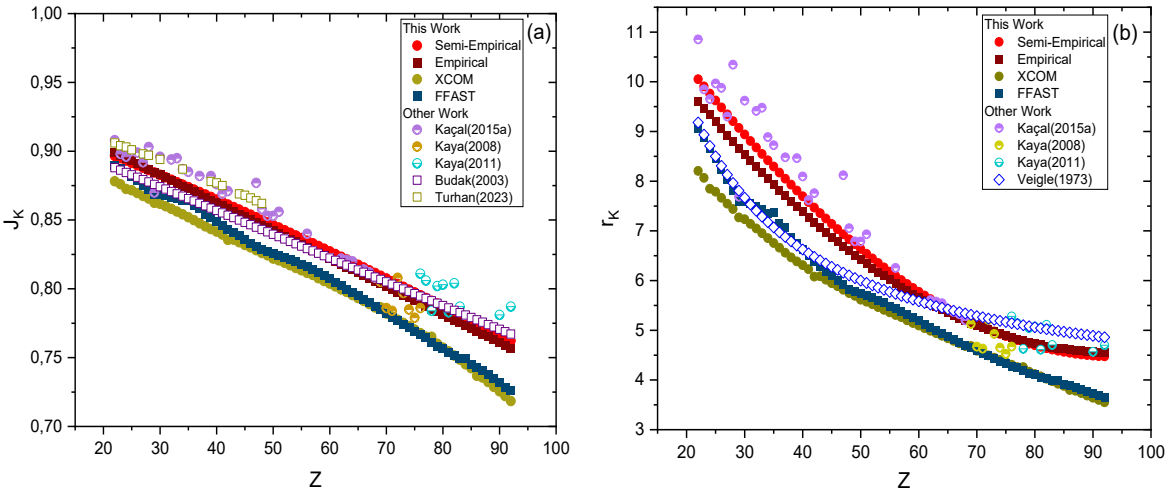
(a)
This Work
Semi-Empirical
Empirical
XCOM
FFAST
Other Work
Kaçal(2015a)
Kaya(2008)
Kaya(2011)
Budak(2003)
Turhan(2023)
J_K
Z
(b)
This Work
Semi-Empirical
Empirical
XCOM
FFAST
Other Work
Kaçal(2015a)
Kaya(2008)
Kaya(2011)
Veigle(1973)
r_K
Z

Fig. 5

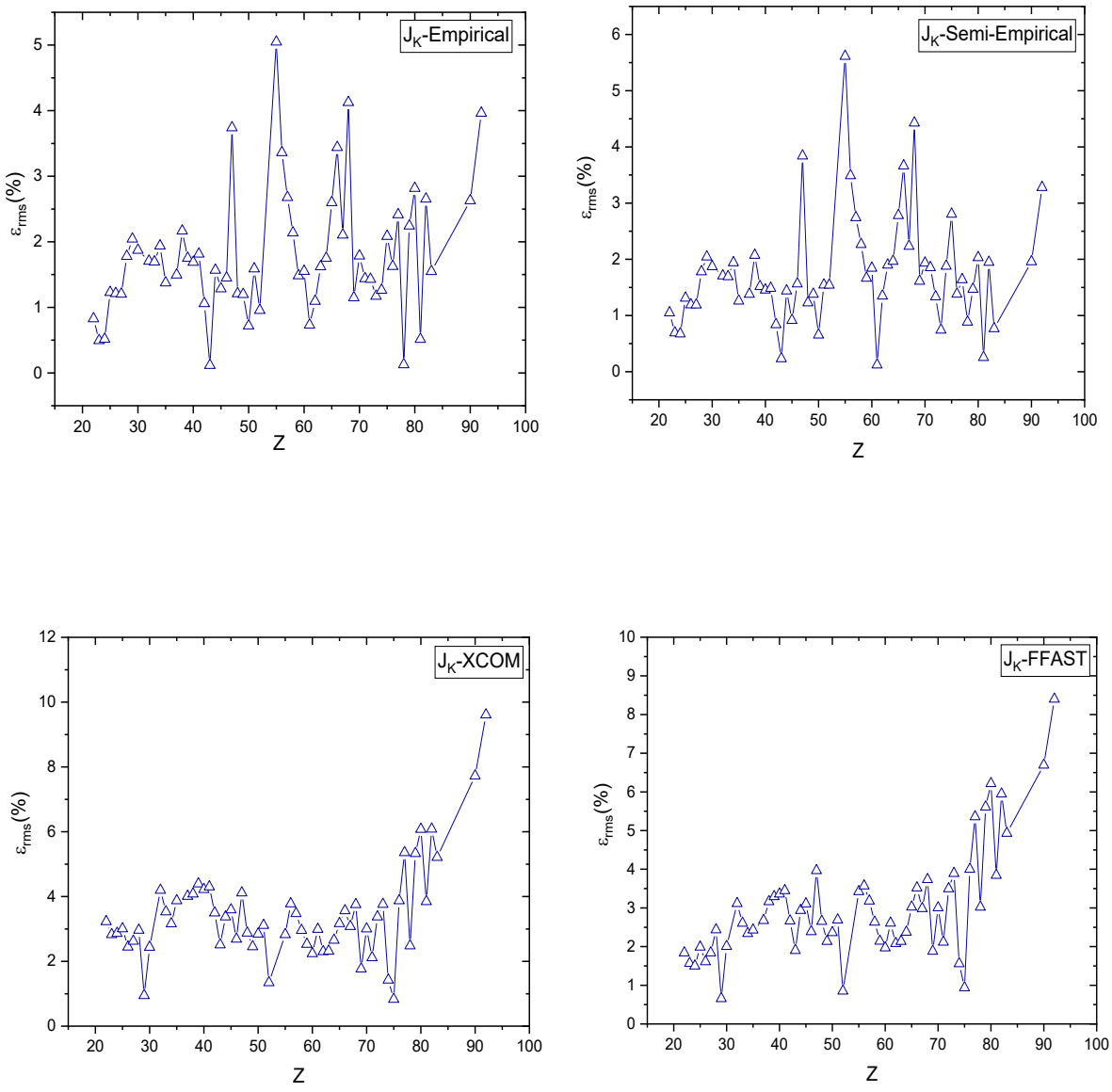

Fig. 6

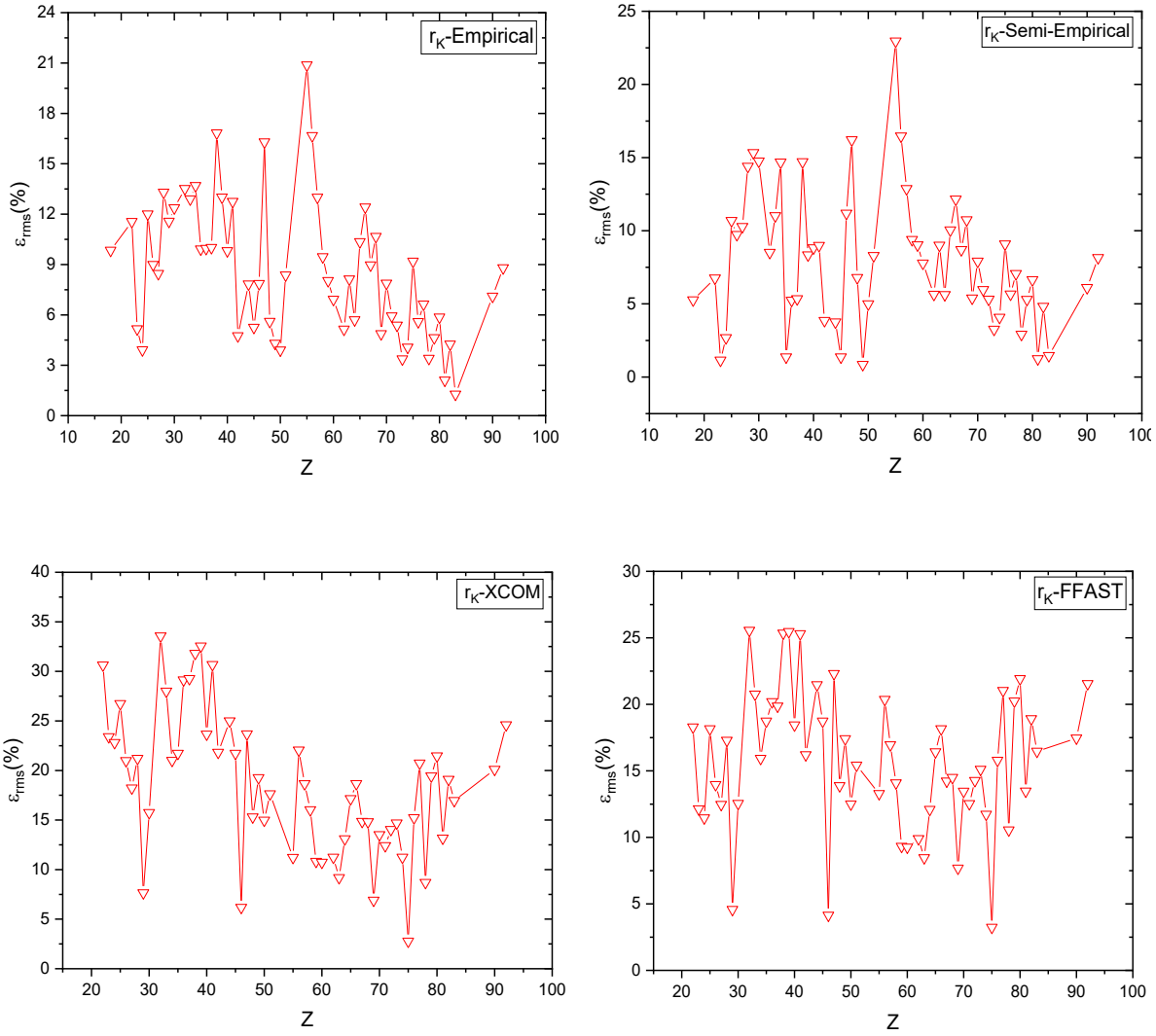
r_K-Empirical
r_K-Semi-Empirical
r_K-XCOM
r_K-FFAST
ε_{rms}(%)
Z

Fig. 7

Table1: Fitting coefficients according to the formulae (6), (7), (9), and (10).

Jump ratio and Factor ratio	Z-range	Function	a_{iJ} , b_{iJ} a_{ir} , b_{ir}	Values
Jump factor	$22 \leq Z \leq 92$	$J_{\mathrm{K-W}}(Z)$	$a_{0\mathrm{J}}$	-0.00201
			$a_{1\mathrm{J}}$	0.94261
		$R_{\mathrm{J}}(Z)$	$b_{0\mathrm{J}}$	0.98875
			$b_{1\mathrm{J}}$	4.9285×10^{-4}
			$b_{2\mathrm{J}}$	-3.3278×10^{-6}
Jump ratio	$18 \leq Z \leq 92$	$r_{\mathrm{K-W}}(Z)$	$a_{0\mathrm{r}}$	14.30159
			$a_{1\mathrm{r}}$	-0.2139
			$a_{2\mathrm{r}}$	0.00116
		$R_{\mathrm{r}}(Z)$	$b_{0\mathrm{r}}$	0.94425
			$b_{1\mathrm{r}}$	0.00246
			$b_{2\mathrm{r}}$	-1.9752×10^{-5}

Table 2. Empirical. semi-empirical. and theoretical (this work) as well as theoretical and experimental (other works) jump factor (J_K) for elements in the range $22 \leq Z \leq 92$.

Z, Element	This work				Other works				
	Empirical	Semi-empirical	Theoretical		fitt	Experimental			
			XCOM	FFAST	(Budak, 2003)	(Kaçal, 2015a)	(Kaya, 2008b)	(Kaya, 2011)	(Turhan, 2023)
Z=22, Ti	0.899	0.897	0.878	0.890	0.888	0.908	-	-	0.906
Z=23, V	0.897	0.895	0.876	0.887	0.886	0.898	-	-	0.904
Z=24, Cr	0.895	0.893	0.873	0.885	0.885	0.896	-	-	0.903
Z=25, Mn	0.893	0.891	0.872	0.882	0.883	0.900	-	-	0.901
Z=26, Fe	0.891	0.890	0.870	0.879	0.881	0.899	-	-	-
Z=27, Co	0.889	0.888	0.867	0.875	0.879	0.892	-	-	0.898
Z=28, Ni	0.887	0.886	0.866	0.872	0.878	0.903	-	-	0.897
Z=29, Cu	0.885	0.885	0.862	0.868	0.876	0.870	-	-	-
Z=30, Zn	0.883	0.883	0.862	0.868	0.874	0.896	-	-	0.894
Z=31, Ga	0.881	0.881	0.860	0.868	0.872	-	-	-	-
Z=32, Ge	0.879	0.879	0.858	0.867	0.871	0.894	-	-	-
Z=33, As	0.877	0.877	0.856	0.865	0.869	0.895	-	-	-
Z=34, Se	0.875	0.876	0.854	0.864	0.867	0.887	-	-	0.887
Z=35, Br	0.873	0.874	0.852	0.864	0.866	0.885	-	-	-
Z=36, Kr	0.871	0.872	0.850	0.860	0.864	-	-	-	-
Z=37, Rb	0.869	0.870	0.848	0.859	0.862	0.882	-	-	-
Z=38, Sr	0.867	0.869	0.845	0.854	0.860	-	-	-	-
Z=39, Y	0.865	0.867	0.843	0.852	0.859	0.882	-	-	0.878
Z=40, Zr	0.863	0.865	0.842	0.849	0.857	0.876	-	-	0.877
Z=41, Nb	0.860	0.863	0.839	0.846	0.855	0.869	-	-	0.875
Z=42, Mo	0.858	0.861	0.836	0.843	0.853	0.871	-	-	0.873
Z=43, Tc	0.856	0.859	0.836	0.841	0.852	0.877	-	-	-
Z=44, Ru	0.854	0.858	0.834	0.838	0.850	-	-	-	0.869
Z=45, Rh	0.852	0.856	0.832	0.836	0.848	-	-	-	0.868
Z=46, Pd	0.850	0.854	0.830	0.833	0.847	-	-	-	0.866
Z=47, Ag	0.848	0.852	0.828	0.831	0.845	-	-	-	0.864
Z=48, Cd	0.846	0.850	0.826	0.828	0.843	0.858	-	-	0.862
Z=49, In	0.844	0.848	0.824	0.827	0.841	0.853	-	-	-
Z=50, Sn	0.842	0.846	0.822	0.826	0.840	0.853	-	-	-
Z=51, Sb	0.840	0.844	0.821	0.825	0.838	0.856	-	-	-
Z=52, Te	0.838	0.843	0.819	0.823	0.836	-	-	-	-
Z=53, I	0.836	0.841	0.817	0.822	0.834	-	-	-	-
Z=54, Xe	0.834	0.839	0.815	0.820	0.833	-	-	-	-
Z=55, Cs	0.832	0.837	0.813	0.818	0.831	-	-	-	-
Z=56, Ba	0.830	0.835	0.812	0.816	0.829	0.840	-	-	-
Z=57, La	0.828	0.833	0.810	0.814	0.828	-	-	-	-
Z=58, Ce	0.826	0.831	0.808	0.812	0.826	-	-	-	-
Z=59, Pr	0.824	0.829	0.806	0.810	0.824	-	-	-	-
Z=60, Nd	0.822	0.827	0.804	0.807	0.822	-	-	-	-
Z=61, Pm	0.820	0.825	0.802	0.805	0.821	-	-	-	-
Z=62, Sm	0.818	0.823	0.800	0.802	0.819	0.822	-	-	-
Z=63, Eu	0.816	0.821	0.798	0.800	0.817	0.821	-	-	-
Z=64, Gd	0.814	0.819	0.795	0.798	0.815	0.820	-	-	-
Z=65, Tb	0.812	0.817	0.793	0.795	0.814	-	-	-	-
Z=66, Dy	0.810	0.815	0.791	0.792	0.812	0.814	-	-	-
Z=67, Ho	0.808	0.813	0.789	0.790	0.810	0.812	-	-	-
Z=68, Er	0.806	0.811	0.786	0.787	0.809	0.808	-	-	-
Z=69, Tm	0.804	0.809	0.786	0.785	0.807	-	0.805	-	-
Z=70, Yb	0.802	0.807	0.782	0.782	0.805	-	0.786	-	-
Z=71, Lu	0.800	0.805	0.780	0.780	0.803	-	0.784	-	-
Z=72, Hf	0.798	0.803	0.778	0.777	0.802	-	0.808	-	-
Z=73, Ta	0.796	0.801	0.775	0.774	0.800	-	0.797	-	-

Z=74, W	0.794	0.799	0.773	0.772	0.798	-	0.785	-	-
Z=75, Re	0.791	0.797	0.770	0.769	0.796	-	0.779	-	-
Z=76, Os	0.789	0.795	0.768	0.767	0.795	-	0.786	0.811	-
Z=77, Ir	0.787	0.793	0.765	0.765	0.793	-	-	0.806	-
Z=78, Pt	0.785	0.791	0.765	0.761	0.791	-	-	0.784	-
Z=79, Au	0.783	0.789	0.760	0.758	0.790	-	-	0.802	-
Z=80, Hg	0.781	0.787	0.757	0.756	0.788	-	-	0.803	-
Z=81, Tl	0.779	0.785	0.754	0.754	0.786	-	-	0.783	-
Z=82, Pb	0.777	0.783	0.751	0.752	0.784	-	-	0.804	-
Z=83, Bi	0.775	0.781	0.748	0.750	0.783	-	-	0.787	-
Z=84, Po	0.773	0.779	0.745	0.749	0.781	-	-	-	-
Z=85, At	0.771	0.777	0.742	0.745	0.779	-	-	-	-
Z=86, Rn	0.769	0.775	0.737	0.743	0.777	-	-	-	-
Z=87, Fr	0.767	0.773	0.736	0.741	0.776	-	-	-	-
Z=88, Ra	0.765	0.771	0.732	0.738	0.774	-	-	-	-
Z=89, Ac	0.763	0.769	0.729	0.735	0.772	-	-	-	-
Z=90, Th	0.761	0.766	0.725	0.732	0.771	-	-	-	-
Z=91, Pa	0.759	0.764	0.722	0.728	0.769	-	-	0.781	-
Z=92, U	0.757	0.762	0.718	0.726	0.767	-	-	0.787	-

Table 3. Empirical, semi-empirical, and theoretical (this work), as well as theoretical and experimental (other works) jump ratio (r_K) for elements in the range $18 \leq Z \leq 92$.

Z, Element	This work				Other works			
	Empirical	Semi-empirical	Theoretical		fitt	Experimental		
			XCOM	FFAST	(Veigele, 1973)	(Kaçal, 2015a)	(Kaya, 2008b)	(Kaya, 2011)
Z=18, Ar	10.197	10.640	-	-	10.444	-	-	-
Z=22, Ti	9.614	10.051	8.207	9.064	9.182	10.852	-	-
Z=23, V	9.473	9.907	8.067	8.879	8.935	9.846	-	-
Z=24, Cr	9.334	9.764	7.848	8.658	8.708	9.652	-	-
Z=25, Mn	9.197	9.623	7.788	8.458	8.500	9.967	-	-
Z=26, Fe	9.062	9.483	7.665	8.239	8.308	9.879	-	-
Z=27, Co	8.929	9.345	7.547	8.025	8.130	9.301	-	-
Z=28, Ni	8.798	9.208	7.439	7.807	7.964	10.345	-	-
Z=29, Cu	8.669	9.073	7.270	7.597	7.810	7.688	-	-
Z=30, Zn	8.542	8.939	7.233	7.592	7.667	9.621	-	-
Z=31, Ga	8.417	8.807	7.141	7.551	7.532	-	-	-
Z=32, Ge	8.294	8.677	7.049	7.499	7.406	9.415	-	-
Z=33, As	8.173	8.548	6.954	7.433	7.288	9.480	-	-
Z=34, Se	8.054	8.421	6.854	7.350	7.176	8.887	-	-
Z=35, Br	7.937	8.296	6.756	7.367	7.071	8.724	-	-
Z=36, Kr	7.822	8.172	6.661	7.155	6.972	-	-	-
Z=37, Rb	7.709	8.050	6.561	7.075	6.878	8.480	-	-
Z=38, Sr	7.598	7.930	6.468	6.865	6.789	-	-	-
Z=39, Y	7.489	7.812	6.385	6.746	6.705	8.463	-	-
Z=40, Zr	7.382	7.696	6.310	6.625	6.625	8.095	-	-
Z=41, Nb	7.277	7.581	6.228	6.503	6.549	7.620	-	-
Z=42, Mo	7.174	7.468	6.080	6.381	6.476	7.760	-	-
Z=43, Tc	7.073	7.357	6.086	6.290	6.407	-	-	-
Z=44, Ru	6.974	7.248	6.017	6.191	6.341	-	-	-
Z=45, Rh	6.877	7.141	5.947	6.097	6.278	-	-	-
Z=46, Pd	6.782	7.036	5.886	6.001	6.217	-	-	-
Z=47, Ag	6.689	6.932	5.816	5.914	6.160	8.120	-	-
Z=48, Cd	6.598	6.831	5.747	5.826	6.104	7.053	-	-
Z=49, In	6.509	6.732	5.693	5.783	6.051	6.789	-	-
Z=50, Sn	6.421	6.634	5.616	5.745	6.000	6.787	-	-
Z=51, Sb	6.336	6.539	5.575	5.701	5.951	6.931	-	-
Z=52, Te	6.253	6.446	5.523	5.652	5.904	-	-	-
Z=53, I	6.172	6.355	5.467	5.607	5.858	-	-	-
Z=54, Xe	6.093	6.265	5.410	5.561	5.815	-	-	-
Z=55, Cs	6.016	6.178	5.361	5.489	5.773	-	-	-
Z=56, Ba	5.940	6.093	5.308	5.437	5.732	6.256	-	-
Z=57, La	5.867	6.010	5.263	5.381	5.693	-	-	-
Z=58, Ce	5.796	5.929	5.199	5.316	5.655	-	-	-
Z=59, Pr	5.727	5.851	5.145	5.254	5.619	-	-	-
Z=60, Nd	5.660	5.774	5.095	5.188	5.583	-	-	-
Z=61, Pm	5.594	5.699	5.043	5.125	5.549	-	-	-
Z=62, Sm	5.531	5.627	4.989	5.059	5.516	5.606	-	-
Z=63, Eu	5.470	5.557	4.941	4.997	5.484	5.576	-	-
Z=64, Gd	5.411	5.489	4.888	4.938	5.453	5.546	-	-
Z=65, Tb	5.353	5.423	4.837	4.875	5.423	-	-	-
Z=66, Dy	5.298	5.359	4.789	4.817	5.394	5.371	-	-
Z=67, Ho	5.245	5.298	4.737	4.759	5.366	5.321	-	-
Z=68, Er	5.194	5.238	4.683	4.702	5.338	5.200	-	-
Z=69, Tm	5.144	5.181	4.684	4.645	5.312	-	5.128	-
Z=70, Yb	5.097	5.126	4.588	4.591	5.286	-	4.673	-
Z=71, Lu	5.052	5.073	4.543	4.537	5.261	-	4.630	-
Z=72, Hf	5.008	5.023	4.495	4.485	5.236	-	5.208	-

Z=73, Ta	4.967	4.974	4.448	4.432	5.212	-	4.926	-
Z=74, W	4.928	4.928	4.402	4.381	5.189	-	4.651	-
Z=75, Re	4.890	4.884	4.356	4.331	5.167	-	4.525	-
Z=76, Os	4.855	4.842	4.306	4.283	5.145	-	4.673	5.278
Z=77, Ir	4.822	4.803	4.259	4.248	5.123	-	-	5.142
Z=78, Pt	4.790	4.765	4.258	4.186	5.103	-	-	4.627
Z=79, Au	4.761	4.730	4.167	4.139	5.082	-	-	5.046
Z=80, Hg	4.733	4.697	4.120	4.104	5.063	-	-	5.072
Z=81, Tl	4.708	4.667	4.073	4.062	5.043	-	-	4.609
Z=82, Pb	4.685	4.638	4.024	4.030	5.024	-	-	5.111
Z=83, Bi	4.663	4.612	3.975	3.992	5.006	-	-	4.704
Z=84, Po	4.644	4.588	3.923	3.985	4.988	-	-	-
Z=85, At	4.626	4.566	3.881	3.919	4.971	-	-	-
Z=86, Rn	4.611	4.546	3.799	3.887	4.953	-	-	-
Z=87, Fr	4.597	4.529	3.781	3.857	4.937	-	-	-
Z=88, Ra	4.586	4.514	3.735	3.811	4.920	-	-	-
Z=89, Ac	4.577	4.500	3.687	3.771	4.904	-	-	-
Z=90, Th	4.569	4.489	3.643	3.729	4.889	-	-	-
Z=91, Pa	4.564	4.481	3.598	3.680	4.874	-	-	4.567
Z=92, U	4.560	4.474	3.552	3.648	4.859	-	-	4.699

Table 4. The root-mean-square error ($\varepsilon_{\mathrm{rms}}\%$) for semi-empirical, empirical and theorical values.

	The root-mean-square error ($\varepsilon_{\mathrm{rms}}\%$)			
	Semi-empirical values	Empirical values	Theorical values	
			XCOM	FFAST
J_{k}	1.787	1.842	3.903	3.456
r_{k}	6.546	8.181	21.881	17.856

Table 5. Theoretical (this work). fit and experimental (other works) oscillator strength (g_K) and Davisson-Kirchner ratio (DK_K) for elements in the range $22 \leq Z \leq 92$.

Z, Element	oscillator strength (g_K)						Davisson-Kirchner ratio (DK_K)			
	This work				Other works		This work		Other works	
	XCOM		FFAST		(Cromer, 1965)	Expérimental			Fitt	Expérimental
	Slope n	g_K	Slope n	g_K			XCOM	FFAST	(Hubbell, 1996)	
Z=22, Ti	2,791	1,211	2.815	1.231	1.360	-	1.139	1.124	1.118	-
Z=23, V	2,775	1,217	2.806	1.230	1.350	-	1.142	1.127	1.121	-
Z=24, Cr	2,787	1,184	2.818	1.212	1.340	-	1.146	1.131	1.124	-
Z=25, Mn	2,749	1,221	2.745	1.256	1.330	-	1.147	1.134	1.127	-
Z=26, Fe	2,767	1,203	2.702	1.282	1.320	-	1.150	1.138	1.130	-
Z=27, Co	2,776	1,191	2.709	1.269	1.310	-	1.153	1.142	1.133	-
Z=28, Ni	2,747	1,205	2.778	1.212	1.310	-	1.155	1.147	1.135	-
Z=29, Cu	2,752	1,180	2.687	1.265	1.300	1.26[a]	1.159	1.152	1.138	1.15[m]
Z=30, Zn	2,733	1,202	2.680	1.271	1.300	-	1.160	1.152	1.140	-
Z=31, Ga	2,748	1,188	2.640	1.298	1.290	-	1.163	1.153	1.143	-
Z=32, Ge	2,716	1,206	2.732	1.223	1.290	-	1.165	1.154	1.145	-
Z=33, As	2,738	1,185	2.729	1.218	1.280	-	1.168	1.155	1.147	-
Z=34, Se	2,732	1,182	2.730	1.209	1.270	-	1.171	1.157	1.150	-
Z=35, Br	2,722	1,182	2.727	1.223	1.270	-	1.174	1.157	1.152	-
Z=36, Kr	2,712	1,181	2.700	1.211	1.260	-	1.177	1.162	1.154	-
Z=37, Rb	2,710	1,174	2.720	1.191	1.260	-	1.180	1.165	1.156	-
Z=38, Sr	2,707	1,170	2.626	1.251	1.250	-	1.183	1.170	1.158	-
Z=39, Y	2,702	1,166	2.647	1.226	1.250	-	1.186	1.174	1.160	-
Z=40, Zr	2,623	1,217	2.633	1.228	1.250	1.19[a]	1.188	1.178	1.162	1.17[m]
Z=41, Nb	2,628	1,205	2.666	1.194	1.240	-	1.191	1.182	1.164	-
Z=42, Mo	2,499	1,284	2.665	1.185	1.240	-	1.197	1.186	1.166	-
Z=43, Tc	2,636	1,189	2.628	1.207	1.240	-	1.197	1.189	1.168	-
Z=44, Ru	2,556	1,244	2.688	1.158	1.230	-	1.199	1.193	1.169	-
Z=45, Rh	2,638	1,175	2.702	1.141	1.230	-	1.202	1.196	1.171	-
Z=46, Pd	2,624	1,180	2.669	1.156	1.230	-	1.205	1.200	1.173	-
Z=47, Ag	2,679	1,135	2.688	1.137	1.230	1.161[a] ,1.19[b]	1.208	1.203	1.175	1.197[b], 1.19[m]
Z=48, Cd	2,629	1,164	2.687	1.129	1.230	1.157[c]	1.211	1.207	1.176	-
Z=49, In	2,558	1,213	2.669	1.134	1.220	-	1.213	1.209	1.178	-
Z=50, Sn	2,562	1,200	2.662	1.133	1.220	1.165[a]	1.217	1.211	1.179	1.19[m]
Z=51, Sb	2,565	1,197	2.650	1.134	1.220	-	1.219	1.213	1.181	-
Z=52, Te	2,627	1,147	2.659	1.120	1.220	-	1.221	1.215	1.183	-
Z=53, I	2,625	1,145	2.659	1.114	1.220	-	1.224	1.217	1.184	-
Z=54, Xe	2,619	1,143	2.629	1.128	1.220	-	1.227	1.219	1.186	-
Z=55, Cs	2,558	1,185	2.647	1.108	1.220	-	1.229	1.223	1.187	-
Z=56, Ba	2,560	1,179	2.641	1.106	1.220	-	1.232	1.225	1.189	-
Z=57, La	2,561	1,174	2.637	1.102	1.220	1.1[c]	1.235	1.228	1.190	-
Z=58, Ce	2,561	1,166	2.649	1.088	1.220	1.057[c] ,1.042[d]	1.238	1.232	1.191	1.214[d]
Z=59, Pr	2,561	1,160	2.632	1.094	1.220	1.015[e]	1.241	1.235	1.193	1.251[e]
Z=60, Nd	2,560	1,156	2.626	1.091	1.220	0.955[e]	1.244	1.239	1.194	1.247[e]
Z=61, Pm	2,559	1,151	2.621	1.089	1.220	-	1.247	1.242	1.196	-
Z=62, Sm	2,549	1,153	2.613	1.088	1.220	1.108[e]	1.251	1.246	1.197	1.247[e]
Z=63, Eu	2,547	1,148	2.613	1.082	1.220	-	1.254	1.250	1.198	-
Z=64, Gd	2,546	1,144	2.621	1.071	1.220	1.060[o]	1.257	1.254	1.199	1.218[n]
Z=65, Tb	2,544	1,139	2.611	1.072	1.220	-	1.261	1.258	1.201	1.266[h]
Z=66, Dy	2,543	1,134	2.608	1.068	1.220	1.046[f]	1.264	1.262	1.202	1.189[f], 1.220[n]
Z=67,Ho	2,544	1,127	2.604	1.064	1.220	-	1.268	1.266	1.203	1.27[h]
Z=68, Er	2,528	1,131	2.601	1.060	1.220	-	1.272	1.270	1.204	1.229[n]
Z=69, Tm	2,527	1,141	2.592	1.060	1.230	-	1.271	1.274	1.206	-
Z=70, Yb	2,525	1,122	2.561	1.075	1.230	1.022[f]	1.279	1.278	1.207	1.217[f]
Z=71, Lu	2,522	1,119	2.576	1.058	1.230	-	1.282	1.283	1.208	1.230[n]
Z=72, Hf	2,519	1,114	2.578	1.051	1.230	1.040[o]	1.286	1.287	1.209	1.236[i]

Z=73, Ta	2,516	1,111	2.555	1.059	1.230	1.010[o]	1.290	1.291	1.210	1.245[i], 1.242[n]
Z=74, W	2,513	1,107	2.557	1.051	1.240	1.039[f]	1.294	1.296	1.212	1.25[g], 1.244[f]
Z=75, Re	2,511	1,103	2.567	1.038	1.240	-	1.298	1.300	1.213	-
Z=76, Os	2,498	1,104	2.561	1.035	1.240	-	1.303	1.305	1.214	-
Z=77, Ir	2,496	1,099	2.560	1.033	1.240	-	1.307	1.308	1.215	-
Z=78, Pt	2,491	1,111	2.578	1.009	1.250	-	1.307	1.314	1.216	-
Z=79, Au	2,487	1,092	2.541	1.025	1.250	-	1.316	1.319	1.217	1.253[i], 1.26[m]
Z=80, Hg	2,482	1,088	2.532	1.026	1.250	-	1.321	1.322	1.218	1.25[g]
Z=81, Tl	2,478	1,084	2.500	1.040	1.250	-	1.325	1.327	1.219	-
Z=82, Pb	2,476	1,077	2.492	1.039	1.250	-	1.331	1.330	1.220	1.28[g] ,1.268[i]
Z=83, Bi	2,475	1,069	2.510	1.018	1.260	-	1.336	1.334	1.221	1.28[g]
Z=84, Po	2,477	1,058	2.505	1.024	1.260	-	1.342	1.335	1.222	-
Z=85, At	2,467	1,059	2.488	1.018	1.270	-	1.347	1.343	1.223	-
Z=86, Rn	2,468	1,036	2.437	1.047	1.270	-	1.357	1.346	1.224	-
Z=87, Fr	2,428	1,068	2.413	1.058	1.270	-	1.360	1.350	1.225	-
Z=88, Ra	2,322	1,145	2.481	1.000	1.280	-	1.366	1.356	1.226	-
Z=89, Ac	2,320	1,135	2.458	1.008	1.280	-	1.372	1.361	1.227	-
Z=90, Th	2,415	1,051	2.443	1.010	1.290	-	1.378	1.366	1.228	1.32[g]
Z=91, Pa	2,408	1,047	2.400	1.033	1.290	-	1.385	1.373	1.229	-
Z=92, U	2,403	1,041	2.417	1.013	1.300	-	1.392	1.378	1.230	1.33[g]

[a](Mallikarjuna et al. 2002)
[b](Niranjana et al. 2013)
[c](Turhan et al. 2018)
[d](Akman et al. 2016a)
[e](Akman et al. 2015b)
[f](Hosur et al. 2011)
[g](Rao et al. 1984)
[h](Niranjina et al. 2015)
[i](Nayak et Badiger. 2006)
[m](Puttaswamy et al. 1981)
[n](Lingam et al. 1989)
[o](Hosur et al. 2008)

Table 6. Theoretical Values (XCOM) and Extrapolated Empirical and Semi-Empirical Results (This Work) for the Jump Factor (J_K), Jump Ratio (r_K), Oscillator Strength (g_K), and Davisson–Kirchner Ratio (DK_K) for Elements with Atomic Numbers $93 \leq Z \leq 100$.

Z, Element	This work								
	Empirical		Semi-Empirical		Theoretical (XCOM)				
	jump factor(J_K)	jump ratio(r_K)	jump factor(J_K)	jump ratio(r_K)	jump factor(J_K)	jump ratio(r_K)	Slope n	oscillator strength (g_K)	Davisson-Kirchner ratio (DK_K)
Z=93, Np	0.755	4.559	0.760	4.470	0.715	3.508	2.313	1.103	1.399
Z=94, Pu	0.753	4.559	0.758	4.467	0.712	3.467	2.311	1.095	1.405
Z=95, Am	0.751	4.562	0.756	4.467	0.708	3.421	2.309	1.086	1.413
Z=96, Cm	0.749	4.566	0.754	4.469	0.704	3.374	2.307	1.077	1.421
Z=97, Bk	0.747	4.572	0.752	4.473	0.700	3.332	2.385	1.006	1.429
Z=98, Cf	0.745	4.581	0.749	4.479	0.696	3.287	2.304	1.048	1.437
Z=99, Es	0.743	4.591	0.747	4.487	0.692	3.242	2.302	1.037	1.446
Z=100, Fm	0.741	4.604	0.745	4.498	0.687	3.198	2.293	1.033	1.455